Chapter 3: Aims of the thesis

3.1) Paediatric caudal epidural block

3.1.1 Dimensions of the neonatal sacrococcygeal membrane

Although the caudal epidural block is commonly performed, some anaesthesiologists find it difficult to determine the correct anatomical location of the sacral hiatus and the caudal epidural space (see Appendix C). Therefore, in order to perform caudal epidural blocks one must first be able to locate the sacral hiatus and also have an understanding of the anatomy of the sacrococcygeal membrane that covers it. This understanding of the landmarks and related structures enables anaesthesiologists to identify the correct point of needle insertion and in turn may increase the success rate of the procedure (Senoglu *et al.,* 2005).

The aim was to record the dimensions of the sacrococcygeal membrane in a sample of neonatal cadavers. Measurements that were taken include the distance between the two sacral cornuae (intercornual distance) and the surface area of the sacrococcygeal membrane.

3.1.2 The distance of the lumbar interlaminar spaces from the apex of the sacrococcygeal membrane in a neonatal sample

An advantage of placing caudal epidural catheters in young children is the fact that it is easier to advance the epidural catheter within the vertebral canal, which can allow for higher positioning of the catheter. This was demonstrated by Bosenberg *et al.* (1988) who, via the caudal route, successfully threaded a catheter to the thoracic levels of children undergoing biliary duct surgery. They believe that this technique could be used as a safe alternative route of access to the thoracic and upper lumber epidural spaces in small infants. In order to select the correct length of the catheter when threading it to higher vertebral levels, anaesthesiologists should be aware of

the possible distances of the apex of the sacrococcygeal membrane (where the catheter is inserted) to the various vertebral levels.

The aims were firstly to measure the distance of the apex of the sacrococcygeal membrane to the inferior border of the interlaminar spaces found between the lumbar vertebrae (L1/L2; L2/L3; L3/L4; L4/L5; and L5/S1) of neonatal cadavers in both a prone and flexed position. Secondly, to determine the percentage change in the distances obtained in the previous aim between the neonate in a prone and flexed position.

3.1.3 The vertebral level of termination and distance from the apex of the sacrococcygeal membrane to the dural sac

Before attempting to perform a caudal epidural block, or inserting a continuous caudal epidural catheter in a paediatric patient, one must have a good understanding of the relevant anatomy of the sacrum and caudal space, as well as the level at which the dural sac ends and the distance from the sacral hiatus (insertion point) to the dural sac. This knowledge is extremely important for anaesthesiologists as it provides an awareness regarding the position of the dural sac when inserting a catheter/needle. The knowledge of the anatomy in turn will increase the level of confidence of the anaesthesiologist performing the block as well as decrease the risk of possible complications, such as dural puncture.

The aim was to measure the distance from the apex of the sacrococcygeal membrane to the dural sac in a sample of neonatal cadavers in a prone position. The vertebral level at which the dural sac ends was also determined by using sagittal MR images of patients ranging from neonates to young adults.

3.2) Paediatric lumbar epidural block

3.2.1 The value of Tuffier's or the intercrestal line in neonates

Using Tuffier's line is the most common method of identifying the correct lumbar interlaminar space when performing lumbar epidural blocks on adults. In infants, this line has been described as crossing the midline at the level of L5/S1 (Jankovic & Wells 2001). Tame and Burstal (2003) evaluated the vertebral level of Tuffier's line in MR images of 35 children less than ten years old and found that Tuffier's line intersected the L5 vertebra. These MR images were evaluated with the children in a neutral position (no flexion of the trunk).

The aims were to determine the vertebral level of Tuffier's line in neonates in a prone position as well as to establish the change in the vertebral level of Tuffier's line when the same sample of neonatal cadavers was flexed.

3.2.2 The dimensions of the lumbar interlaminar spaces in neonates in both a prone and flexed position

Research regarding the dimensions of the interlaminar space is limited. Boon and co-workers (2003) found, from measuring the dimensions of the adult lumbar vertebrae, that the L3/L4, L4/L5, and L5/S1 interlaminar spaces becomes significantly smaller with increased age. All measurements were taken on articulated vertebral columns in an erect position. A search of the available literature showed no mention of the dimensions of the lumbar interlaminar spaces in neonates. This knowledge could be of benefit to anaesthesiologists performing lumbar epidural blocks or spinal anaesthesias on neonates or physicians doing lumbar punctures on neonates to obtain CSF samples.

The aims were to determine the surface area of the interlaminar spaces between vertebral levels L1/L2, L2/L3, L3/L4, L4/L5, and L5/S1 in neonatal cadavers in both a prone and flexed position, and secondly, to determine the percentage change that occurs in the measurements between the neonate in a prone and flexed position.

3.2.3 The vertebral level and distance from the apex of the sacrococcygeal membrane of the conus medullaris

Knowledge of the position of the end of the spinal cord or conus medullaris in both children and adults is of utmost importance for anaesthesiologists performing neuraxial or central blocks and physicians performing lumbar punctures. Direct trauma to the spinal cord may occur if the needle is inserted too deeply, at higher vertebral levels. Although this is a rare complication, as most punctures are carried out inferior to the conus medullaris (Jankovic & Wells, 2001), insufficient knowledge of neonatal anatomy and incorrect identification of the needle insertion point may cause trauma to the spinal cord. Neurological disorders may result from the insertion of the tip of the needle into the spinal cord, especially if the local anaesthetic solution is injected. This could tear the nerve fibres and/or produce compression lesions, possibly with severe consequences (Dalens, 1995).

The aims were therefore to first ascertain at which vertebral level the spinal cord terminates (conus medullaris) in a sample of (a) neonatal cadavers and (b) sagittal MR images. Secondly, to determine the distance of the apex of the sacrococcygeal membrane to the conus medullaris on neonatal cadavers.

3.3) Paediatric infraclavicular approach to the brachial plexus

3.3.1 Anatomical considerations of the neonatal infraclavicular brachial plexus block

Most anatomical research is based on investigations and techniques originally performed on adults. Although the success rate of these studies were good, either a nerve stimulator or other expensive imaging modalities were used to identify the brachial plexus. The use of these modalities has shown to increase the success rate of these regional blocks dramatically (Rapp & Grau, 2004; Minville *et al.*, 2005; Bloc *et al.*, 2006; McCormack & Malherbe, 2008; Aziz *et al.,* 2009). Even with the aid of nerve stimulators or CT guidance, no regional anaesthetic technique could truly be called simple, safe and consistent until the anatomy has been closely examined (Winnie *et al.*, 1975). After an extensive search of the literature regarding brachial plexus blocks in a paediatric population, it is clear that there is surprisingly little research available on the anatomy of the paediatric brachial plexus and how it relates to the different infraclavicular block techniques.

The first aim was to determine the relationship of the brachial plexus (and its components), within the axilla, to the coracoid process. The second aim was to use the data obtained to determine an improved needle insertion site for the infraclavicular brachial plexus block using the coracoid process and the xiphisternal joint as easily identifiable bony landmarks. The final aim was to determine the distance of the inserted needle from the parietal pleura when performing the infraclavicular approach on a neonatal cadaver population in order to ascertain the risk of pneumothorax.

3.3.2 Anatomical considerations of the infraclavicular brachial plexus block–comparison between neonatal and adult data

A search of the literature revealed that very little information regarding the anatomy of the brachial plexus is available. Katz (1993) stated that "except for the absence of subcutaneous fat in children, the anatomy of the neurovascular bundle in the infraclavicular and axillary regions are *presumed* to be essentially the same as in adults. The depth of the brachial plexus is shallower in children". Even using modern imaging, Birchansky & Altman (2000) could not accurately describe the brachial plexus in paediatric patients and ultimately concluded that "imaging the plexii and peripheral nerves of infants and children are a challenging endeavour, which is at the cutting edge of current MR imaging technology". As a result anaesthesiologists have applied their knowledge of adult anatomy, which is far more readily available, when performing brachial plexus blocks in neonates and young infants. This is clearly summarised in Table 3.1.

Table 3.1: Summary of cases where the infraclavicular brachial plexus blocks were performed on paediatric patients.

Author	Sample size	Age of sample	Technique used	Original sample
De Jose Maria & Tielens, 2004	55	5–17	Kilka *et al.,* 1995	Adults
Fisher *et al.,* 2006	1	10	Fisher *et al.,* 2006	Child
Dadure *et al.,* 2003	2	6 & 11	Jandard *et al.,* 2002	Adults
Fleischmann *et al.,* 2003	40	1–10	Kapral *et al.,*1996	Adults
Zimmermann *et al.,* 2002	1	8	Kilka *et al.,* 1995	Adults
Marhofer *et al.,* 2004	40	1-10	Fleischmann *et al.,* 2003 (Kapral *et al.,* 1996)*	Adults*

* Marhofer *et al.* (2004) used the infraclavicular block technique described by Fleischmann *et al*. 2006, which was originally developed by Kapral *et al.,* 1996.

If the assertions made by Katz (1993) are correct, then performing procedures on paediatric patients that was originally designed on adults shouldn't be a problem. One cannot just assume that this is the case. There is

very little scientific evidence to prove that there are no differences between the position of and relationship between the structures found in the axilla when comparing paediatric and adult populations.

The aims were therefore to firstly determine the relationship of the brachial plexus (and its components), within the axilla, to the coracoid process. The second aim was to use the data obtained to determine an improved needle insertion site for the infraclavicular brachial plexus block using the coracoid process and the xiphisternal joint as easily identifiable bony landmarks. The third aim was to determine the distance of the inserted needle from the parietal pleura when performing the infraclavicular approach on an adult cadaver population in order to determine the risk of pneumothorax when performing this procedure. The final aim was to compare the data obtained in the adult sample to that found in the neonatal sample (see *5.3.1: Anatomical considerations of the neonatal infraclavicular brachial plexus block*).

3.4) Paediatric femoral nerve block

3.4.1 Anatomical considerations of the neonatal femoral nerve block

Although there is no mystery regarding the femoral nerve and its position within the femoral triangle, there are still relatively few studies of the anatomy of the nerve in children, especially neonates. Classical anatomical literature describes the femoral artery as entering the femoral triangle, posterior to the inguinal ligament, at the mid-inguinal point. The femoral nerve can then be found between 5mm–10mm lateral to the artery in children (Dalens, 2003). This is despite the fact that no anatomical studies have been conducted on a paediatric sample to verify this.

The aim was therefore to determine the accurate position of the femoral nerve, in relation to the femoral artery and the ASIS and PT, within the femoral triangle of a neonatal sample.

3.4.2 Anatomical considerations of the femoral nerve block– comparison between neonatal and adult data

Femoral nerve blocks are well established as a peripheral nerve block in adult patients. To immediately assume that the position of the contents of the femoral triangle will be exactly the same in neonates as in adults would be a mistake.

Therefore, the aim was to compare the position of the neonatal femoral nerve and artery, within the femoral triangle, to the position of the adult nerve and artery. This was accomplished by conducting a similar study as described in *5.4.1: Anatomical considerations of the neonatal femoral nerve block* on an adult population.

3.5) Paediatric ilio-inguinal/ iliohypogastric nerve block

3.5.1 Anatomical considerations of the neonatal ilio-inguinal/ iliohypogastric nerve block

Although inguinal hernia repair is one of the most common surgical procedures performed on neonates and premature infants, the precise anatomical positions of both the ilio-inguinal and the iliohypogastric nerves have not been identified in this age group. Knowledge of the exact anatomical location of these nerves would enhance the success of this block, which carries a relatively high failure rate in this age group (Trotter *et al.*, 1995; Eichenberger *et al.*, 2006).

The primary aim was to establish the anatomical position of the ilio-inguinal and iliohypogastric nerves in relation to an easily identifiable bony landmark, the ASIS, and the secondary aim was to evaluate three techniques - described in the literature - from an anatomical perspective.

3.6) Problem statement

It is inadvisable to use data obtained from adult studies and use it on neonates, infants and even toddlers. This is due to the fact that the relationship of the targeted nerve to surrounding anatomical landmarks differs significantly from that of adults. It would therefore be more appropriate to use data obtained from neonatal samples and extrapolate “up” when performing regional nerve blocks on infants and even toddlers.

Chapter 4: Materials & Methods

4.1) Paediatric caudal epidural block

4.1.1 Dimensions of the neonatal sacrococcygeal membrane

The sacrococcygeal membrane, as well as the sacral cornuae was carefully exposed in a sample of 40 neonatal cadavers (mean length: 0.42m ± 0.07m; mean weight: 1.59kg ± 0.85kg). Both sacral cornuae and the apex of the sacrococcygeal membrane, or the upper margin of the sacral hiatus, were identified and pins were placed into each of these landmarks. High quality digital photographs were then taken of the sacral area. A scale of known distance was placed on top of the dissected area (without covering any of the relevant structures) in order to make digital measurements of the photograph possible. The photographs were then imported into *UTHSCSA* Image Tool V3.0, which was used to analyse the photographs. Using the *Calibrate Spatial Measurements* function, the known scale found on each photograph was converted into a pixel format. This allows for accurate measurement of the photographs by means of the *Distance* function, which converts the length of a straight line – drawn between two points on the photograph – into mm. These measurements were then inserted into an MS Excel™ worksheet and subsequent statistical analysis of the data was done.

The digital photographs were used to measure (a) the distance between the sacral cornuae, (b) the length of the sacrococcygeal membrane (distance between an imaginary line drawn between the two sacral cornuae and the apex of the sacrococcygeal membrane). The *Area* function was used to determine the surface area of the sacrococcygeal membrane, which consisted of a triangular area between the two sacral cornuae (base) and the apex of the sacral hiatus (see Figure 2.1).

4.1.2 The distance of the lumbar interlaminar spaces from the apex of the sacrococcygeal membrane in a neonatal sample

The lumbar and sacral regions of 40 neonatal cadavers (mean length: 0.42m ± 0.07m; mean weight: 1.59kg ± 0.85kg) were carefully dissected in order to expose the laminae and spinous processes of the lumbar vertebrae and sacrum.

With the exposure of the lumbar vertebrae and sacrum a pin was inserted into the apex of the sacrococcygeal membrane as well as the inferior border of the interlaminar spaces found between L1/L2; L2/L3; L3/4; L4/L5 and L5/S1 (see Figure 4.1).

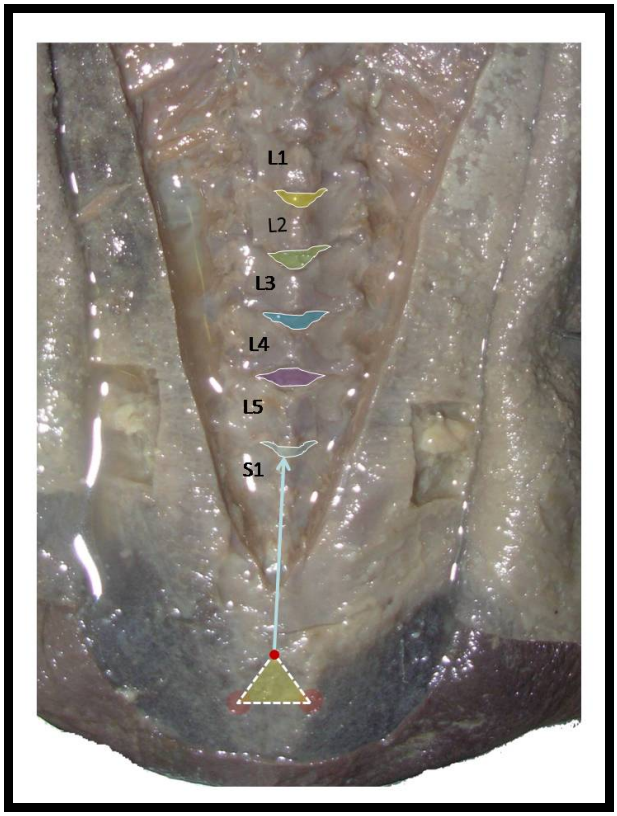

Figure 4.1: Exposed lumbar vertebrae and apex of sacrococcygeal membrane (yellow triangle) of a neonate in the prone position.

Measurements were taken from the apex (red circle) to the inferior border of the interlaminar spaces between each of the lumbar vertebrae (highlighted in colour). Dissection above shows measurement from the apex to the inferior border of the L5/S1 interlaminar space.

Digital photographs were taken with the neonate placed in a prone position as well as with the neonate flexed between 40^{o}-50^{o} over a wooden block. These photographs were then imported into UTHSCSA Image Tool V3.0 to measure the distance of the apex of the sacrococcygeal membrane to the inferior borders of the interlaminar spaces of L1/L2; L2/L3; L3/4; L4/L5 and L5/S1 in both a prone and flexed position.for analysis.

The data obtained from the neonate in both a prone and flexed position was then inserted into a MS Excel™ worksheet in order to determine the change that occurs in these measurements between the neonate in a prone and flexed position. The percentage change of the distance of the apex of the sacrococcygeal membrane to the inferior border of the interlaminar spaces between the lumbar vertebrae was determined for each neonate in both a prone and flexed position. The distances in a prone position (α) was divided by the distances in the same neonate in a flexed position (β) and then multiplied by a hundred to obtain a percentage (θ). This percentage was then subtracted from a hundred in order to obtain the percentage change between the two positions. Thus, **$\theta = (\alpha / \beta) \times 100$** and then the **% change = 100 – θ**

For example:
θ = (17.04mm / 19.13mm) x 100
θ = 0.8907 x 100
θ = 89.07% change = 100 – 89.07
Therefore, % change = 10.93%

4.1.3 The vertebral level of termination and distance from the apex of the sacrococcygeal membrane to the dural sac

Firstly, the lumbar and sacral regions of 40 neonatal cadavers (mean length: 0.42m ± 0.07m; mean weight: 1.59kg ± 0.85kg) were carefully dissected in order to expose the laminae and spinous processes of the lumbar vertebrae and sacrum. Prior to dissecting the laminae, a pin was placed at the

apex of the sacrococcygeal membrane and care was taken not to disturb it during the dissection.

Using a scalpel, both the laminae of the sacrum and the lumbar vertebrae were cut and the spinous processes were carefully removed, effectively exposing the dural sac within the vertebral canal (see Figure 4.2). A second pin was placed at the point were the dural sac ended.

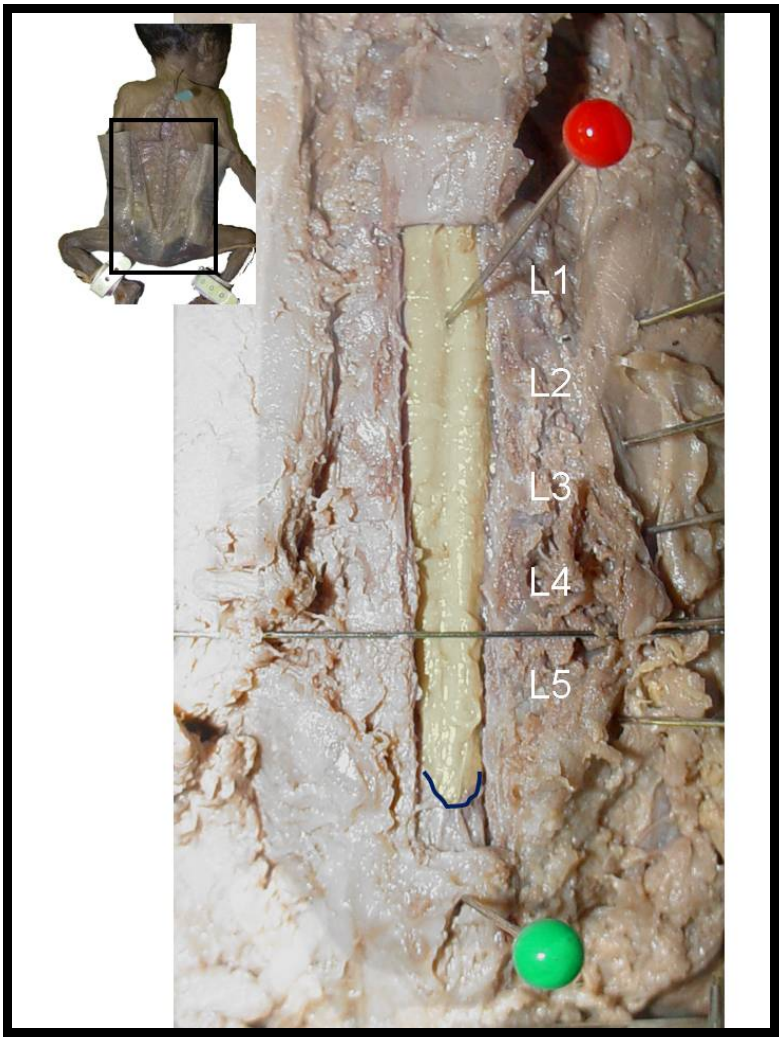

Figure 4.2: Content of the vertebral canal

The laminae and spinous processes were removed in order to show the dural sac (highlighted in yellow). The green pin has been placed into the apex of the sacrococcygeal membrane, while the red pin was placed into the L1/L2 interlaminar space prior to removal of the laminae and spinous process of the lumbar vertebrae. The end of the dural sac is indicated by the curved black line.

High quality digital photographs were taken of the exposed dural sac and were then imported into UTHSCSA Image Tool V3.0 to determine the distance of the apex of the sacrococcygeal membrane (marked by the green pin) to the end of the dural sac.

In order to determine the vertebral level where the dural sac ends, a series of 102 midsagittal T2-weighted MR images of the lumbar and sacral regions (patients' ages ranging between 1 day to 29 years old) was analysed.

Each vertebra on the MR image was divided into thirds and each third, as well as each intervertebral disc was given a corresponding number, i.e., the upper third of T12 was "1", the middle third of T12 was "2", the lower third of T12 was "3" and the T12/L1 intervertebral disc was "4". Numbering then continued from the upper border of L1 (which was "5") to the lower third of S3 (which was number "35") (see Figure 4.3). The level at which the dural sac ended was noted on the MR images and given a corresponding number.

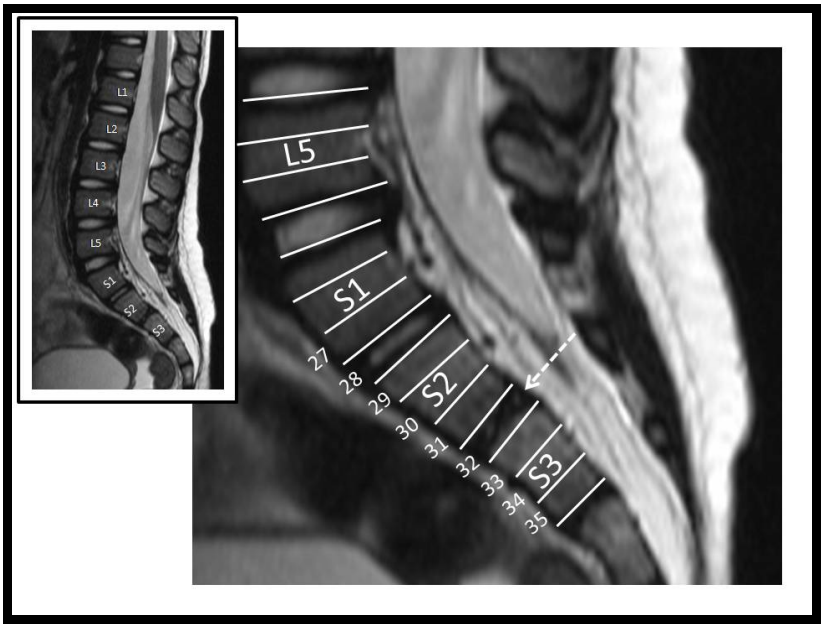

Figure 4.3: MR image of a 2 year old showing how the vertebrae were divided into thirds.

Each third as well as the intervertebral disc was then given a corresponding number. The end of the dural sac (indicated by the white, dashed arrow).

4.2) Paediatric lumbar epidural block

4.2.1 The value of Tuffier's or the intercrestal line in neonates

The lumbar and sacral regions of 40 neonatal cadavers (mean length: 0.42m ± 0.07m; mean weight: 1.59kg ± 0.85kg) were carefully dissected in order to expose the laminae and spinous processes of the lumbar vertebrae. During dissection, the two iliac crests were also exposed and the most superior border of each iliac crest was marked. Each vertebra was divided into thirds. Each third, as well as each interlaminar space, was given a corresponding number, i.e., the upper third of T12 was "1", the middle third of T12 was "2", the lower third of T12 was "3" and the T12/L1 intervertebral disc was "4". Numbering then continued from the upper border of L1 (which was "5") to the L5/S1 intervertebral disc (which was number "24"). High quality digital photographs were taken of the dissected vertebral column in both a prone and a flexed position. Using imaging software, a straight line was drawn between the two marked iliac crests. The vertebral level (indicated by a corresponding number) where this line intersected the vertebral column was then noted in both positions (see Figure 4.4).

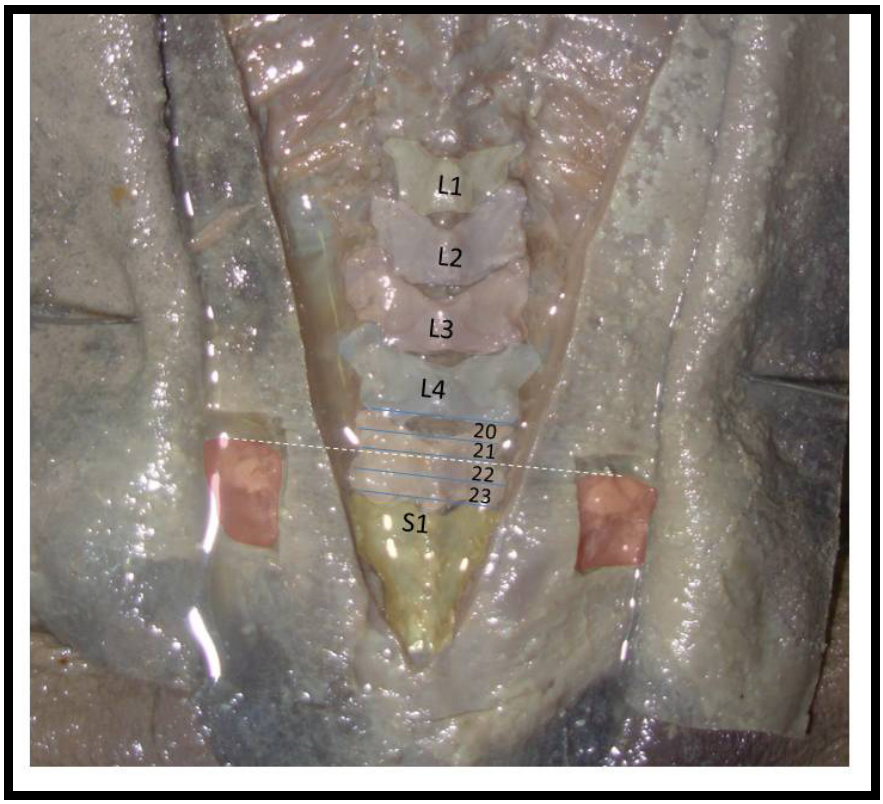

Figure 4.4: The exposed lumbar vertebrae of a neonatal cadaver in a prone position.

The vertebral bodies (divided into thirds) and interlaminar space was each given a corresponding number (in the picture above the L4/L5 interlaminar space and L5 vertebral body is divided and numbered 20-23). The two iliac crests were also exposed and a line was drawn between these two bony landmarks (indicated by the white dashed line).

The photographs were imported into *UTHSCSA* Image Tool V3.0 to determine the distance of the apex of the sacrococcygeal membrane (marked by a pin) to Tuffier's line in both a prone and a flexed position.

The percentage change of the distance of the apex of the sacrococcygeal membrane to Tuffier's line was determined for each neonate in both positions by using the principle discussed in *4.1.2: The distance of the lumbar interlaminar spaces from the apex of the sacrococcygeal membrane in a neonatal sample.*

.

4.2.2 The dimensions of the lumbar interlaminar spaces in neonates in both a prone and flexed position

The lumbar and sacral regions of 40 neonatal cadavers (mean length: 0.42m ± 0.07m; mean weight: 1.59kg ± 0.85kg) were carefully dissected in order to expose the interlaminar spaces of the lumbar vertebrae. High quality digital photographs were taken of the dissected vertebral column of the neonatal sample, in both a prone and a flexed position, and were then imported into UTHSCSA Image Tool V3.0 for analysis. This allowed for accurate measurements of the surface area of the interlaminar spaces between L1/L2, L2/L3, L3/L4, L4/L5 and L5/S1.

The percentage change of the surface area of the interlaminar space of a neonate in a prone and flexed position was then determined by using the principles discussed in *4.1.2: The distance of the lumbar interlaminar spaces from the apex of the sacrococcygeal membrane in a neonatal sample.*

4.2.3 The vertebral level and distance from the apex of the sacrococcygeal membrane of the conus medullaris

4.2.3.1 Neonatal cadavers

The lumbar and sacral regions of 40 neonatal cadavers (mean length: 0.42m ± 0.07m; mean weight: 1.59kg ± 0.85kg) were carefully dissected in order to expose the laminae and spinous processes of the lumbar vertebrae and sacrum. Prior to dissecting the laminae, a pin was placed at the apex of the sacrococcygeal membrane and care was taken not to disturb it during the dissection. The lumbar vertebrae were carefully marked for future reference.

Using a scalpel, both the laminae of the sacrum and the lumbar vertebrae were cut and the spinous processes carefully removed, effectively exposing the dural sac within the vertebral canal (see Figure 4.2). A midline incision was made through the dural sac and the two halves of the now transected dural sac was reflected laterally in order to expose the spinal cord and cauda equina (see Figure 4.5).

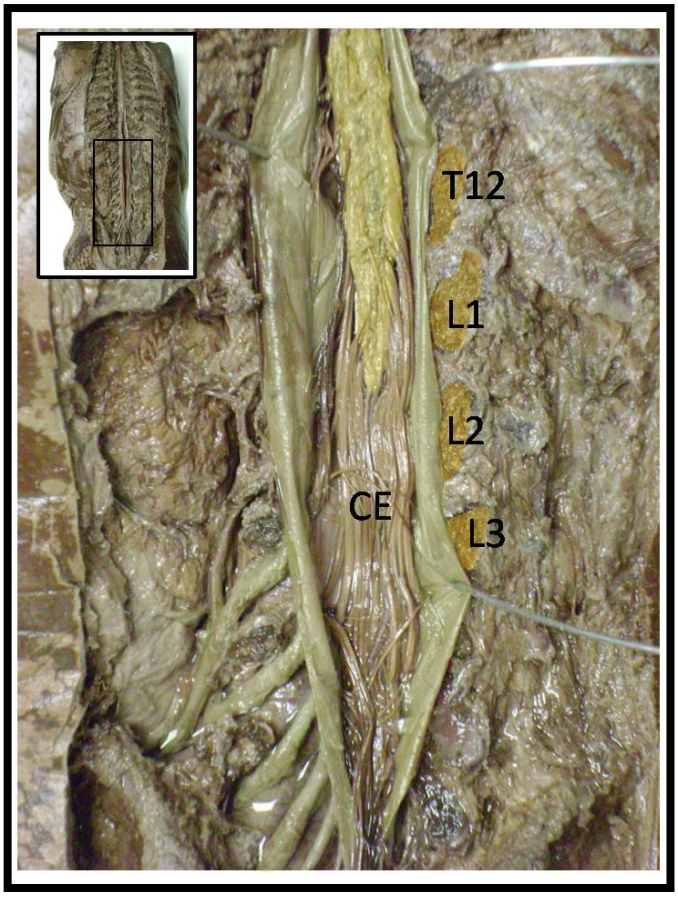

Figure 4.5: An exposed spinal cord (highlighted in yellow) of a neonatal cadaver.

The T12-L3 vertebrae (highlighted in orange) are also indicated. The dura mater (highlighted in green was sectioned and reflected in order to show the spinal cord and cauda equina (CE).

High quality digital photographs were taken of the dissected vertebral columns of the neonatal sample, in both a prone and a flexed position, and were then imported into UTHSCSA Image Tool V3.0 to determine the distance from the apex of the sacrococcygeal membrane (marked by a pin) to the conus medullaris in both positions.

The percentage change of the distance of the apex of the sacrococcygeal membrane to the conus medullaris was determined for each neonate in both a prone and flexed position, by using the principles discussed in *4.1.2: The distance of the lumbar interlaminar spaces from the apex of the sacrococcygeal membrane in a neonatal sample.*

Each vertebra was also divided into thirds and each third as well as each intervertebral disc was given a corresponding number similar to that shown in Figure 4.6. After exposing the spinal cord, a pin was placed at the level of termination of the conus medullaris, the vertebral level was noted and a corresponding number was given. This was done on 39 neonatal cadavers, all in the prone or neutral position.

4.2.3.2 MR images

In order to determine the vertebral level where the spinal cord ends, a series of 108 midsagittal T2-weighted MR images of the lumbar and sacral regions (patients' ages ranging between 1 day to 29 years old) was obtained, with the appropriate ethical clearance, from Burger Radiologists, UNITAS hospital and the Department of Radiology, Steve Biko Academic Hospital.

Each vertebra on the MR image was divided into thirds and each third as well as each intervertebral disc was given a corresponding number as can be seen in *4.1.3: The vertebral level of termination and distance from the apex of the sacrococcygeal membrane to the dural sac.*

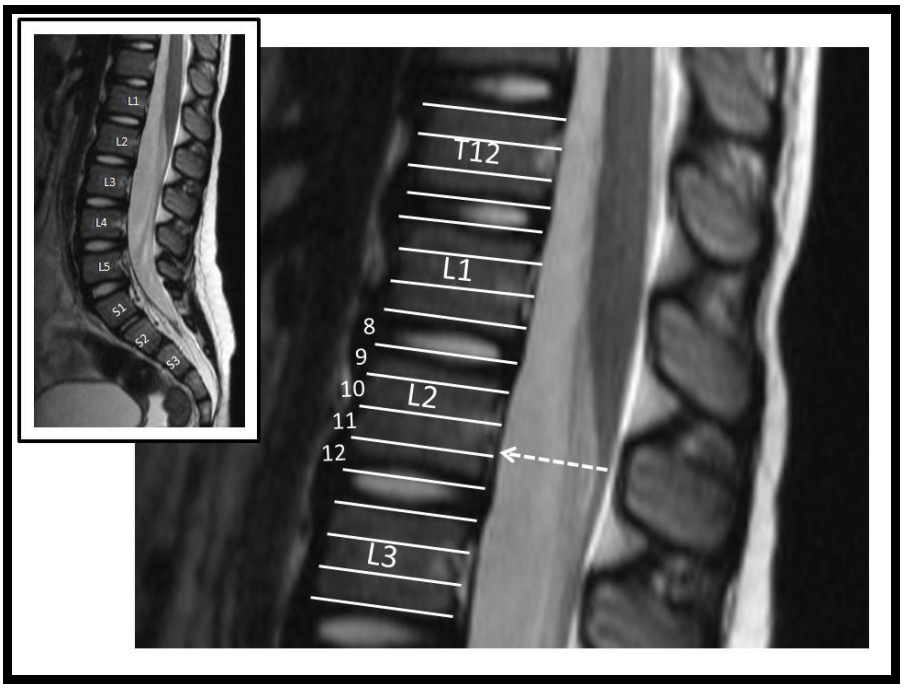

Figure 4.6: MR image of a 2 year old showing how the vertebrae were divided into thirds.

Each third as well as the intervertebral disc was then given a corresponding number. The end of the spinal cord (indicated by the white, dashed arrow) was then given a number corresponding with the vertebral level of termination.

4.3) Paediatric infraclavicular approach to the brachial plexus

4.3.1 Anatomical considerations of the neonatal infraclavicular brachial plexus block

The content of the axilla was carefully exposed in a sample of 52 neonatal cadavers (52 left and 50 right axillae; mean length: 0.43m ± 0.08m; mean weight: 1.94kg ± 1.62kg). The skin over the pectoral region was first removed in order to expose the pectoralis major muscle (see Figure 4.7), and subsequently reflect it in order to expose the underlying pectoralis minor muscle (see Figure 4.8).

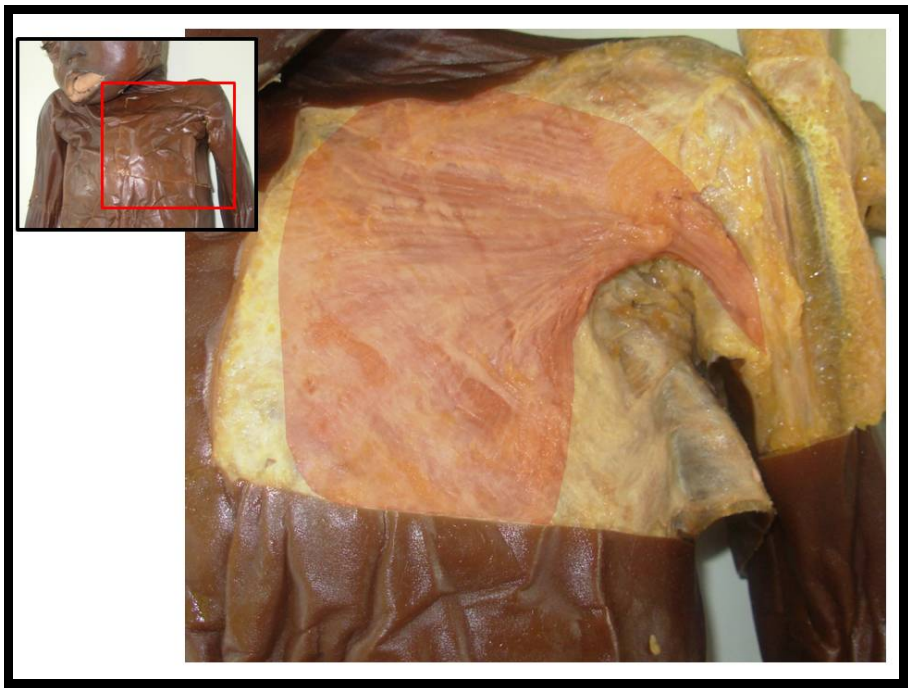

Figure 4.7: Skin reflected from the pectoral region of a neonatal cadaver in order to expose the pectoralis major muscle.

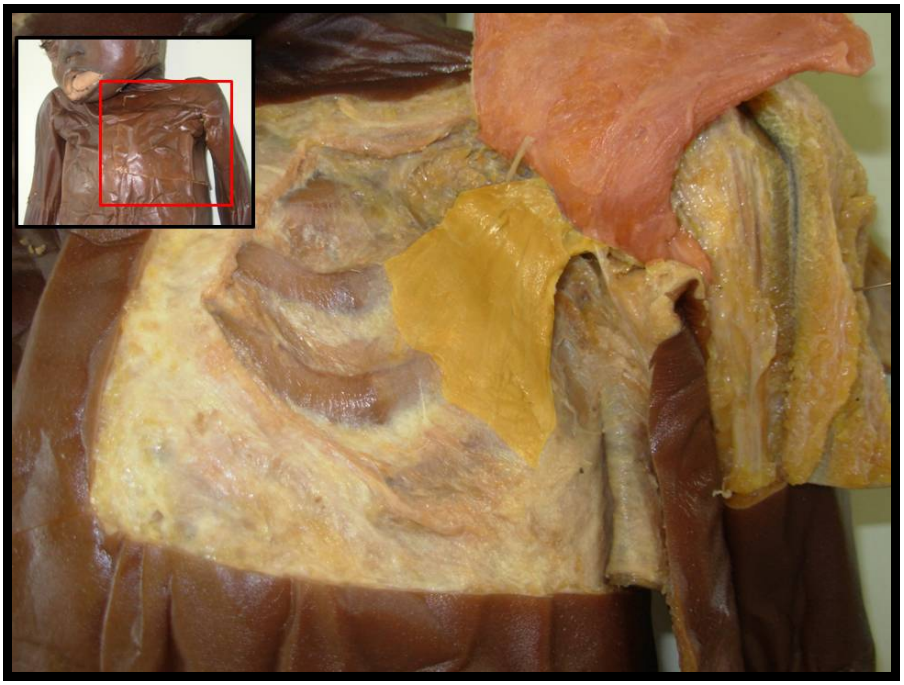

Figure 4.8: Pectoralis major muscle (highlighted in red) reflected in order to expose the pectoralis minor muscle (highlighted in orange).

Care was taken not to disturb the structures within the axillary sheath when the pectoralis minor was reflected (see Figure 4.9a & b). The axillary vein was carefully removed in order to better visualise the structures of the axilla. All measurements were done with the cadavers' arms adducted and supinated, lying against the trunk. The distance between (a) the coracoid process and the xiphisternal joint (CP-XS line) was measured using a mechanical dial sliding calliper (accuracy of 0.01mm).

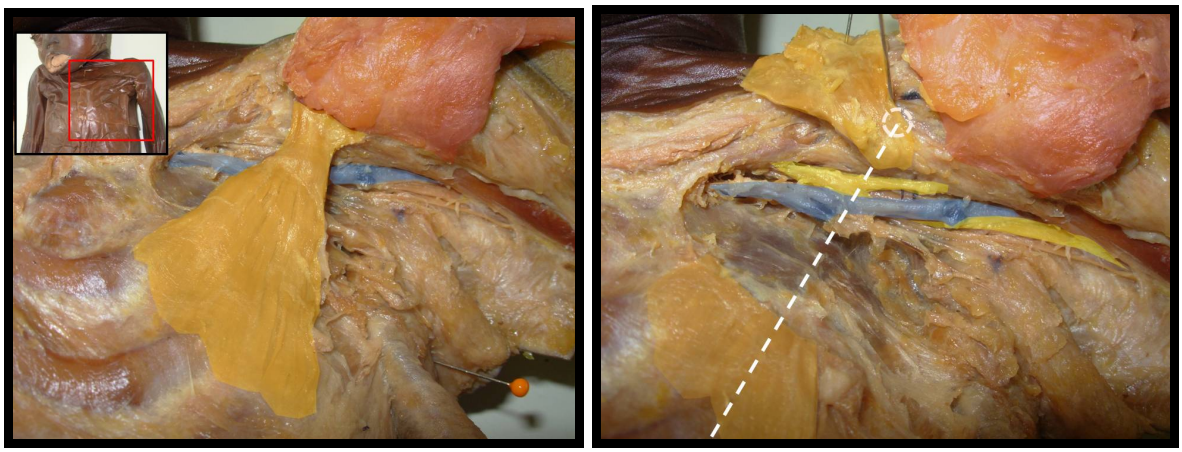

(a) **(b)**

Figure 4.9a: Pectoralis minor muscle.

Pectoralis major muscle (highlighted in red) reflected in order to expose the pectoralis minor muscle (highlighted in orange) with content of the axilla traversing posterior to it. The axillary vein, the most superficial structure in the axillary sheath, is highlighted in blue.

Figure 4.9b: Content of the axilla.

Both the pectoralis major muscle (highlighted in red) and the pectoralis minor muscle (highlighted in orange) has been reflected in order to expose the axillary sheath. The axillary vein and brachial plexus (lateral cord and some terminal branches are visible) are highlighted in blue and yellow respectively. The position of the coracoid process is indicated by the dashed circle, while the CP–XS line is indicated by the white dashed line.

The distances of the coracoid process to (b) the lateral cord of the brachial plexus (LBP) and (c) medial cord of the brachial plexus (MBP) were then measured on the CP-XS line, as well as (d) the distance between the LBP and MBP. These distances were then converted to a percentage of the

CP-XS line distance and recorded in an MS Excel™ worksheet where further statistical analysis was done, i.e., distance of the coracoid process to the LBP (%)=100(measurement **b** / measurement **a**) and the distance of the MBP (%)=100(measurement **c** / measurement **a**). The midpoint of between the LBP and MBP, along the CP-XS line was also determined as this should be the ideal point of needle insertion. Therefore the point of needle insertion should be (e) the measurement **b** + ½ measurement **d** (see Figure 4.10).

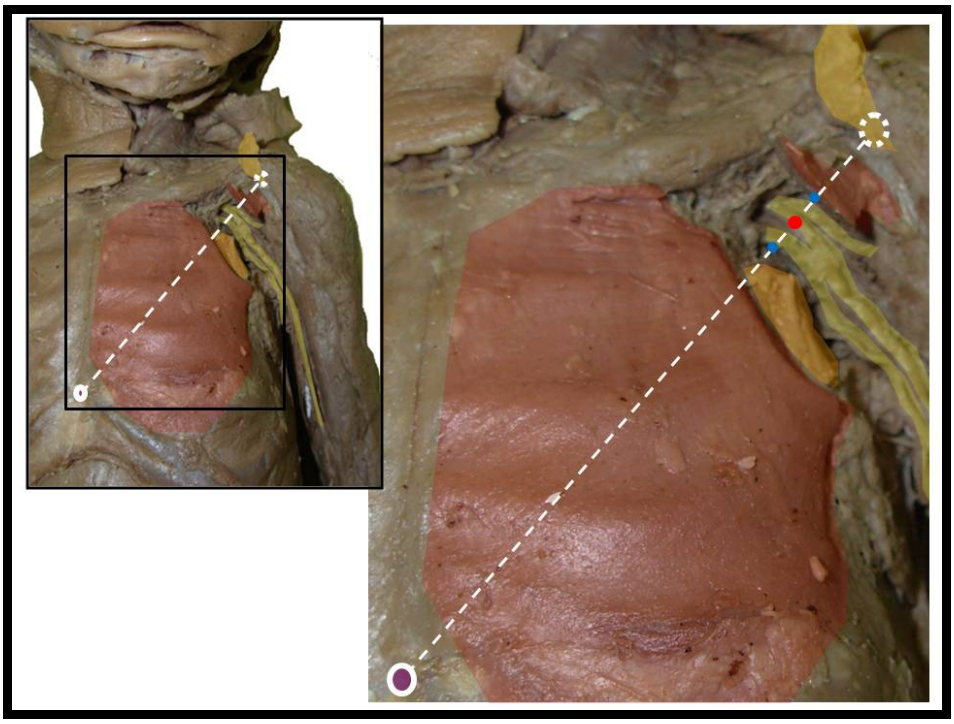

Figure 4.10: Schematic of measurements taken on exposed brachial plexus.

Both the pectoralis major and minor muscles (highlighted in red and orange respectively) have been reflected in a neonatal cadaver in order to expose the brachial plexus (highlighted in yellow). The red circle indicates the ideal site for needle insertion, or the point halfway between the LBP and MBP (blue circles) on the CP–XS line (white dashed line, between the coracoid process (dashed circle) and the xiphisternal joint (purple circle with white border).

A paired *t*-test was performed to compare the all the results from the right side of the adult sample to that of the left side.

A Pearson's correlation coefficient test (correlation coefficient or R) was conducted to determine correlation coefficient or the strength of the correlation between the dependent and independent variables. In this study the

dependent variables were (a) the distance from the coracoid process to the point of needle insertion and (b) the distance from the coracoid process to the point of needle insertion as a percentage of the CP–XS line distance. The independent variables were the length, weight and CP–XS line distances of the sample.

In the cases where a strong correlation existed between two variables ($R > 0.7$), the coefficient of determination (or R^2) was determined, which is a statistical measure of how well the regression line approximates the real data points. In these cases, a linear regression formula was developed with the distance from the CP to the point of needle insertion along the CP–XS line, as the *dependant variable* and the CP–XS line distance (mm) as the *independent variable*.

The distance of (f) the MBP to the closest rib was also measured to determine the closest distance between the possible position of the needle and the thoracic wall, and subsequently the pleural cavity. All measurements were done with the cadavers' arms adducted and supinated, lying against the trunk.

4.3.2 Anatomical considerations of the infraclavicular brachial plexus block–comparison between neonatal and adult data

Similar to *4.3.1: Anatomical considerations of the neonatal infraclavicular brachial plexus block*, the content of the axilla was carefully exposed in a sample of 81 adult cadavers (74 left and 70 right axillae; mean length: 1.70m ± 0.09m; mean weight: 57.57kg ± 14.95kg) and measurements were taken with a mechanical dial sliding calliper (accuracy of 0.01mm).

In order to compare the results of the neonatal sample (see *5.3.1: Anatomical considerations of the neonatal infraclavicular brachial plexus block)* with the above adult sample, a paired *t*-test was performed on measurements (b)–(d). Only the values given as a percentage of the CP-XS line distance were compared as the distances in millimetres quite clearly shows a difference between neonates and adults, due to the large size

differences and not because of differences of the position of the brachial plexus within the axilla.

4.4) Paediatric femoral nerve block

4.4.1 Anatomical considerations of the neonatal femoral nerve block

In order to visualise the specific anatomical structures, i.e., femoral artery, nerve, PT and ASIS, the skin and subcutaneous fat covering the anterior abdominal wall and femoral triangle was reflected in both sides of 54 neonatal cadavers (50 left and 50 right; mean length: 0.44m ± 0.08m; mean weight: 1.96kg ± 1.57kg). Needles were then inserted into the specific bony landmarks (ASIS and PT), as well as into the centre of the femoral artery and femoral nerve (at a point immediately inferior to the inguinal ligament) (see Figure 4.11). Four separate measurements (i–iv) were then made on both the left and right sides of each cadaver using a mechanical dial sliding calliper. Measurements were taken from (i) the ASIS to the PT, (ii) the ASIS to the femoral nerve, (iii) the ASIS to the femoral artery, and (iv) the femoral artery to the femoral nerve.

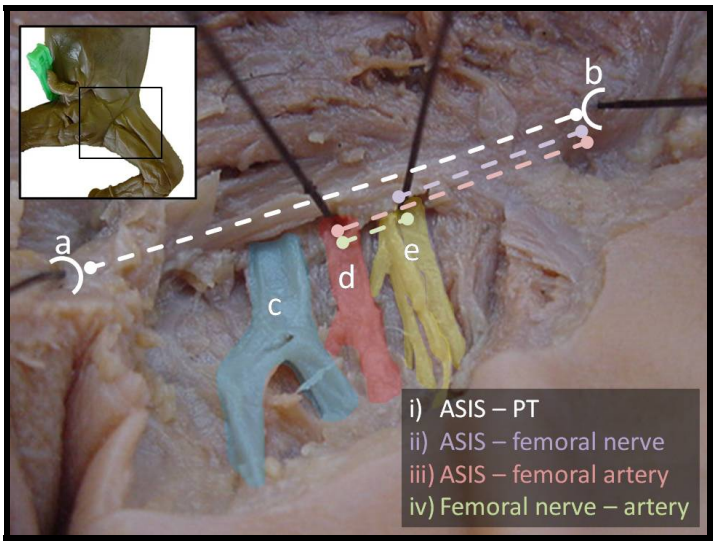

Figure 4.11: Neonatal femoral triangle.

Needles were placed into the (a) PT, (b) ASIS, (c) femoral vein, (d) femoral artery and (d) femoral nerve. The dashed lines indicate the measurements that were taken.

After all measurements were taken, the distances of the femoral nerve (ii) and artery (iii) was converted to a percentage of the ASIS-PT line distance (i), i.e., femoral nerve (%) = 100(ii / i) and the femoral artery (%) = 100(iii / i). This would allow for determining at what point (as a percentage of the ASIS-PT line distance) the femoral nerve and artery passes posterior to the inguinal ligament to enter the femoral triangle.

A paired *t*-test was performed to compare all the results from the two sides.

A Pearson's correlation coefficient test (correlation coefficient or R) was conducted to determine the correlation coefficient or the strength of the correlation between the dependent variables, i.e., the distance from the ASIS to the femoral nerve in mm and as a % of the ASIS-PT line distance, and the independent variables, the length, weight and ASIS-PT line distance (i) of the sample.

In the cases where a strong correlation (R > 0.7) existed between the two variables, a linear regression formula together with the coefficient of determination (or R^2) was determined.

4.4.2 Anatomical considerations of the femoral nerve block– comparison between neonatal and adult data

The skin and subcutaneous fat covering the anterior abdominal wall and femoral triangle was reflected on each side of 77 adult cadavers. Similar to that of the neonatal sample (see *4.4.1 Anatomical considerations of the neonatal femoral nerve block*), measurements and statistical analyses were done on the adult sample.

The data obtained from the adult sample was then compared to the data obtained in the neonatal sample (see *5.4.1: Anatomical considerations of the neonatal femoral nerve block)* using a paired *t*-test.

4.5) Paediatric ilio-inguinal/ iliohypogastric nerve block

4.5.1 Anatomical considerations of the neonatal ilio-inguinal/ iliohypogastric nerve block

A midline incision through the skin stretching from the umbilicus to the pubic symphysis as well as two horizontal incisions laterally from the umbilicus and pubic symphysis was made bilaterally in a sample of 54 neonatal cadavers (51 left and 53 right sides; mean length: 0.43m±0.06m; mean weight: 1.64kg±0.72kg). The skin was then reflected laterally, leaving the superficial fascia of the anterior abdominal wall intact. The superficial fat layer was carefully removed to expose the superficial muscles and the rectus sheath of the anterior abdominal wall (see Figure 4.12).

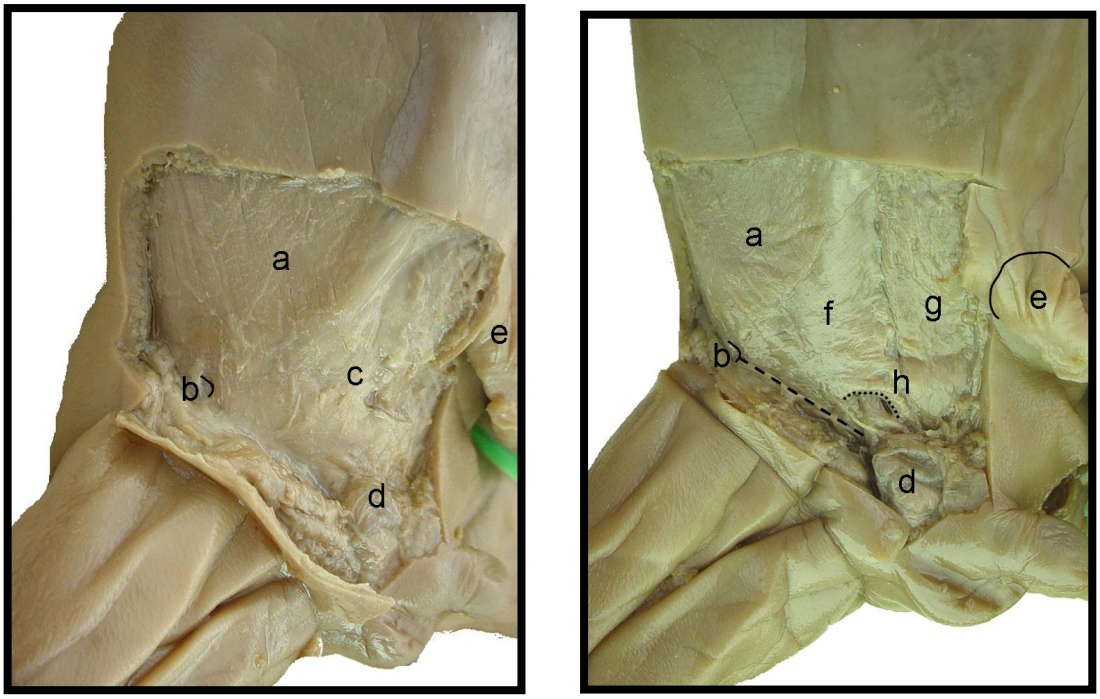

Figure 4.12: Superficial and deeper dissections of the anterior abdominal wall of a neonatal cadaver.

Structures that are visible include the external oblique muscle (a), the ASIS (b), the rectus sheath (c), testis (d), the umbilicus (e), internal oblique muscle (f), rectus abdominis muscle (g), and the conjoint tendon (h) (also indicated with the smaller, curved dotted line). The inguinal ligament is indicated with a dashed line.

A midline incision was made through the external oblique muscle and then carefully reflected laterally to expose the underlying internal oblique muscle. The ilio-inguinal nerve was then identified as it coursed through the deeper layers and travelled within the inguinal canal (see Figure 4.13). The nerve was then followed superolaterally to the point where it penetrates the internal oblique muscle. The latter was then carefully removed in sections to expose the course of the ilio-inguinal nerve back to a point superolateral to the ASIS. The iliohypogastric nerve, which courses superior to the ilio-inguinal nerve, was exposed in a similar manner (see Figure 4.14).

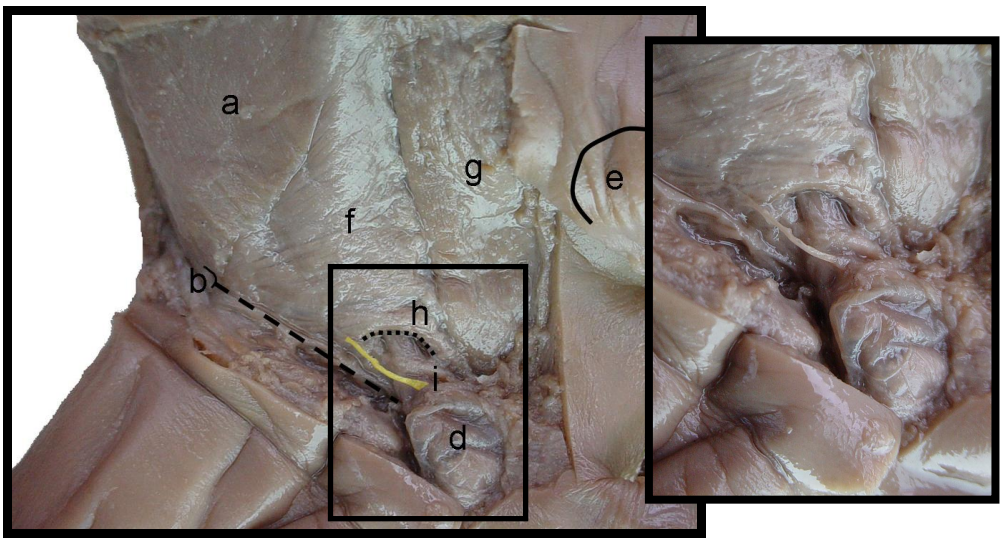

Figure 4.13: Dissection of anterior abdominal wall and the ilio-inguinal nerve.

The nerve can be seen piercing the internal oblique muscle (f) running with the spermatic cord towards the testis (d). Other structures include the external oblique muscle (a), ASIS (b), umbilicus (e), rectus abdominis muscle (g), conjoint tendon (h) (also indicated with the smaller, curved dotted line), and the ilio-inguinal nerve (i).

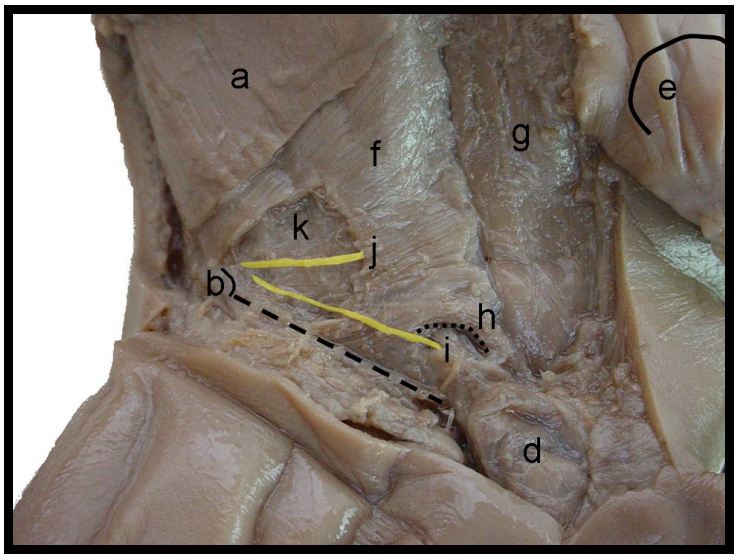

Figure 4.14: Dissection of the anterior abdominal wall and the ilio-inguinal and iliohypogastric nerves.

As the nerves pass inferomedial past the ASIS (b), they are still running in the plane between the transversus abdominis (k) muscle and internal oblique muscle (f). Other structures include the external oblique muscle (a), testis (d), umbilicus (e), rectus abdominis muscle (g), conjoint tendon (h) (also indicated with the smaller, curved dotted line), the ilio-inguinal nerve (i) and iliohypogastric nerve (j).

The ASIS was identified on both sides and the distance of both nerves from the ASIS - on a line connecting the ASIS to the umbilicus - was measured with a mechanical dial sliding calliper (accuracy of 0.01mm).

After complete dissection and identification of the nerves, a needle was then inserted according to the methods described by Von Bahr (1979) (see Figure 2.15), Sethna and Berde (1989) (see Figure 2.16) and Schulte-Steinberg (1990) (see Figure 2.17). The respective positions of the needle and its relationship to the nerves were documented for each specimen dissected.

Statistical analysis included a comparison between the left and right sides by using a paired *t*-test.

A Pearson's correlation coefficient test (correlation coefficient or R) was conducted to determine the correlation coefficient or the strength of the correlation between the dependent variables, i.e., the distance of the ilio-inguinal and iliohypogastric nerves from the ASIS and the distance of the point

of needle insertion from the ASIS, and the independent variables, the length and weight of the sample population.

In the cases where a strong or high, moderate correlation ($R > 0.6$) between the dependent and independent variables was found, the coefficient of determination (or R^2) was determined. This is a statistical measure of how well the regression line, that was also determined, approximates the real data points.

4.6) Sample size and selection

In order to obtain the relevant data, three separate sample populations were used. These were: (a) neonatal cadavers, (b) adult cadavers, and (c) MR images.

4.6.1 Neonatal sample

A total of 69 neonatal and two infant cadavers, stored in the Department of Anatomy of the University of Pretoria (n = 60) and University of the Witwatersrand (n = 11), were selected for this study. The ages of the cadavers ranged from stillborn babies to 2-month-old. The mean weight of the neonatal sample was 1.77kg and it included very low birth weight cadavers (less than 1.5kg), low birth weight cadavers (less than 2.5kg) and normal birth weight cadavers (more than 2.5kg). The mean length of the cadavers was 0.43m ± 0.07m (mean ± SD). The University of the Witwatersrand's sample of cadavers were only used for the femoral nerve and ilio-inguinal/ iliohypogastric nerve blocks.

4.6.2 Adult sample

A total of 90 adult cadavers, stored at the Department of Anatomy of the University of Pretoria, were used as a basis for comparison with the neonatal data. The mean age of the adult sample was 61 years ± 20 years. The samples age ranged between 23 years and 94 years. The mean weight of the sample was 57.53kg ± 15.49kg and the mean length was 1.70m ± 0.09m.

The adult sample was used in the femoral nerve and infraclavicular blocks to compare with the data obtained from the neonatal sample.

4.6.3 MRI scans

A total of 108 T-2 weighted midsagittal lumbar MR images were obtained from Burger Radiologists, UNITAS hospital and the Department of Radiology, Steve Biko Academic Hospital. The MRI scans were used for the lumbar and caudal epidural blocks.

4.7) Ethical considerations

Ethical approval to conduct this study was obtained from the Ethics Committee of the University of Pretoria. All dissections of the neonatal and adult cadavers were performed in accordance with the Human Tissue act 65 of 1983 (Government Gazette, 1983).

Permission to access MR images was obtained from Burger Radiologists, UNITAS Hospital and the Department of Radiology, Steve Biko Academic Hospital.

4.8) Statistical analysis

All measurements were entered into MS Excel™. Statistical analysis of all the measurements and subsequent comparisons of these measurements with the demographic profile of both the sample of neonatal cadavers and MRI scans were performed using Statistix™ Ver. 8.0 for Windows.

In certain cases where a linear correlation between two variables are expected (i.e., distance to a nerve will increase with the length of the patient), a Pearson's correlation coefficient test (correlation coefficient or R) was conducted to determine the strength of the correlation between the dependent variable and the independent variables. This test determines the strength of the linear relationship between two variables ($R < 0.3$ is considered to be a weak correlation, $R = 0.3 – 0.7$ is considered to be a moderate correlation, and $R > 0.7$ is considered to be a strong correlation between the variables). In the cases where a moderate or strong correlation was found, a linear regression formula was determined.

Linear regression is a method of estimating the conditional expected value of one variable (dependent variable) when the values of another variable or variables (independent variables) are known. The dependant and independent variables will be discussed in more detail in each separate Chapter.

The coefficient of determination (or R^2) was determined for any linear regression model with a strong or high, moderate correlation between the dependant and independent variables. R^2 is a statistical measure of how well the regression line "fits"; in other words, how well the dependant variable is "explained" by the independent variables in the model. For example, a value such as $R^2 = 0.7$ may be interpreted that approximately seventy percent of the variation in the dependent variable can be explained by the independent variable. The remaining thirty percent can be explained by unknown variables or inherent variability.

4.9) Limitations of the study

The small sample size and the fact that mostly neonatal cadavers were used are directly related to the scarcity of paediatric cadavers of different age groups. Data on neonatal cadavers is however equally rare and therefore immensely valuable.

Shrinkage is a common artefact and occurs during preservation of cadavers. Although the shrinkage is minimal, it should nevertheless be taken into account when data is obtained from the neonatal cadavers.